



# Antibiofouling thin-film composite membranes (TFC) by in situ formation of Cu-(*m*-phenylenediamine) oligomer complex

B. Rodríguez<sup>1</sup> , D. Oztürk<sup>1</sup> , M. Rosales<sup>1,2</sup> , M. Flores<sup>3</sup> , and A. García<sup>1,\*</sup>

<sup>1</sup>Advanced Mining Technology Center (AMTC), Universidad de Chile, Av. Tupper 2007, 8370451 Santiago, Chile

<sup>2</sup>Laboratory of Nanoscale Materials, Department of Materials Science, Universidad de Chile, Beauchef 851, 8370456 Santiago, Chile

<sup>3</sup>Physics Department, Faculty of Physics and Mathematics Sciences, Universidad de Chile, 8370415 Santiago, Chile

Received: 28 August 2017

Accepted: 14 January 2018

Published online:  
23 January 2018

© Springer Science+Business  
Media, LLC, part of Springer  
Nature 2018

## ABSTRACT

In situ formation of a Cu-(*m*-phenylenediamine) (Cu-mPD) oligomer complex from copper chloride during the interfacial polymerization process was successfully employed to produce modified thin-film composite reverse osmosis membranes (TFC-RO) with antibiofouling properties. Membranes were characterized by field emission scanning electron microscopy, Fourier transform infrared spectroscopy (FTIR), X-ray photoelectron spectroscopy (XPS), X-ray diffraction (XRD), atomic force microscopy, and contact angle measurements. Antibiofouling properties were studied using a colony-forming unit test with *Escherichia coli*. Moreover, an antiadhesion test was developed using fluorescence microscopy. Membrane performance using a cross-flow cell was evaluated, and copper concentration in permeate water was measured. FTIR, XPS and XRD results confirmed the formation of a Cu-mPD oligomer complex and its incorporation into the polyamide layer. A mechanism for formation of the oligomer within the membrane was proposed based on the interaction between the oxygen of the carbonyl group of the polyamide layer and copper ion of the Cu-mPD oligomer complex. The modified membrane showed a slight decrease in hydrophilicity and higher surface roughness. However, excellent antibacterial and antiadhesion effects were observed, attributed to copper toxicity as a result of Cu<sup>2+</sup> ions release from the membrane surface. Release of copper ions in the permeate water was determined, and the maximum value observed was considered negligible according to the World Health Organization. The desalination performance of modified membrane showed an important salt rejection with stable water flux. In conclusion, a novel chemical method for the incorporation of Cu-mPD oligomer complex into the polyamide layer of TFC-RO membranes to improve their antibiofouling properties and desalination performance was achieved.

Address correspondence to E-mail: andreina.garcia@amtc.cl

## Introduction

Water scarcity has been the driving force behind many researchers' focus on development of suitable methods to obtain freshwater from saltwater and ways to reuse water in order to sustain future generations. Therefore, membrane-based processes are considered key components of water treatment and desalination technologies and the reliability of these membranes systems has led to an increase in their use [1–5].

The best known polymer membranes for reverse osmosis (RO) with applications in desalination processes are made from an aromatic polyamide group of polymers mainly known as thin-film composite (TFC). TFC-RO membranes consist of an ultrathin PA layer obtained by the reaction between diamine in water phase and acyl chloride in organic phase on a porous polysulfone. An example of a reaction for the formation of polyamide layer can be derived from *m*-phenylenediamine (MPD) and trimesoyl chloride (TMC). These TFC membranes dominate the RO membrane field at present because of their excellent water flux and solute rejection capabilities, but they are not completely resistant to fouling [1, 2, 5–7].

Membrane fouling is considered one of the most critical issues affecting seawater desalination plants. It is an inevitable obstacle in the process that causes a decrease in membrane performance, which consequently increases operational and maintenance costs [1, 2]. Membrane fouling can be broadly categorized into three categories: (1) inorganic; (2) organic; and (3) biofouling [7]. In the case of biofouling, it is caused by the attachment and proliferation of microorganism communities on the membrane surface; these eventually form a biopolymer matrix or complex structure, which is considered a biofilm, on the membrane surface [7]. Severe biofouling can produce significantly decreased flux, compromised separation performance, cleaning frequency, product contamination, accelerated membrane damage, and aging [8]. Biofouling formation can be influenced by membrane surface properties due to physical and chemical interactions between the membrane and foulants. Properties such as hydrophilicity, roughness and electrostatic charge are considered [9–11]. Most studies concerning enhancement of TFC-RO membrane properties have involved the introduction of hydrophilic layers, the reduction in surface

roughness, and the introduction of negative surface charges. One of the alternatives to obtain these benefits is through the modification of membrane surface by incorporating inorganic nanomaterials [12–15]. For example, incorporation of conventional nanomaterials such as titanium dioxide (TiO<sub>2</sub>), silicon dioxide (SiO<sub>2</sub>), zeolites, and silver (Ag) nanoparticles in addition to the emerging carbon-based nanomaterials such as carbon nanotubes (CNT) and graphene into desalination membranes in order to improve the antibiofouling properties and desalination performance of RO membranes has been developed [16, 17].

On the other hand, the modification of these membranes with antimicrobial nanoparticles could also improve the antibiofouling effect by inactivation of bacteria on the membranes surface upon contact with the toxic nanoparticles or due to the nanoparticles acting as source releasing ion biocide into the boundary layer above the membrane [18–20].

In this way, the incorporation of copper has also been investigated considering their germicidal properties [21–23]. Copper shows exceptionally good antimicrobial properties and has been reported to be highly effective against a wide variety of bacteria, fungi, and microalgae [24–28]. Thus, both copper ions and nanoparticles have been used for modifying ultrafiltration, nanofiltration, reverse osmosis (RO) membranes and vacuum membrane distillation, in order to enhance their antibiofouling properties [18, 19, 29–36].

Nevertheless, optimal copper incorporation methods into TFC-RO membranes have been a challenge. For example, commercial RO membranes modified with adsorbed copper hydroxide (Cu(OH)<sub>2</sub>) particles [18], polyamide (PA) functionalization with Cu nanoparticles (Cu-NPs) made by dip coating [19], or in situ surface functionalization with Cu-NPs formed on the surface of commercial TFC-RO membranes [32] have been developed. Moreover, incorporation of CuO nanoparticles within the PA layer of TFC-RO membranes during the interfacial polymerization process has also been reported [37, 38]. However, in situ formation of copper nanoparticles within the PA layer of the TFC-RO membranes produced during interfacial polymerization reaction have not yet been reported.

It has also been reported that a Cu-poly-*m*-phenylenediamine (Cu-PmPD) nanocomposite can be prepared by directly mixing aqueous solutions of copper salts, an oxidizing agent and mPD. A Cu-

mPD oligomer complex with nanoparticle structures is formed as a suitable intermediate in order to activate polymerization and induce morphology evolution of the PmPD nanostructures before the mPD polymerization. A complete mPD conversion is achieved in the presence of an oxidizing agent and a long reaction time [39, 40].

Thus, Cu-mPD oligomer complex structures formed in short time periods and characterized as intermediates in the synthesis of Cu-PmPD composites are materials loaded with copper ions [41], and they can be used as charged compounds to produce materials with potential antibiofouling properties. In this way, in situ formation of the Cu-mPD oligomer complex within the PA layer of TFC-RO membranes during the interfacial polymerization reaction can be a novel alternative for development of antibiofouling RO membranes.

Owing to the above-mentioned facts, we have proposed a novel and easy method for incorporating the Cu-mPD oligomer complex within the PA membranes of the TFC membranes during the interfacial polymerization process. This method uses direct mixing of aqueous solutions of copper salts and mPD for a short period of time prior to the reaction with TMC. The mechanism of Cu-loaded mPD oligomer formation and incorporation into the membrane has been proposed, and the antibiofouling effect and desalination performance of modified membrane have also been studied.

## Materials and methods

### Materials

The PSf support was produced from Udel P-3500 MB7-Solvay Advanced Polymers (in pellet form, MW: 83000 g/mol) employing 1-methyl-2-pyrrolidone (NMP, > 99.5% purity, Sigma-Aldrich) and *N,N*-dimethylformamide (DMF, > 99% purity, Sigma-Aldrich) as solvents. The PSf support was obtained using the phase inversion method [23, 34] according to the previously reported method [28]. The PA layer was synthesized from mPD monomers and TMC, which were obtained from Sigma-Aldrich.  $\text{CuCl}_2$  powder (99%), NaOH (> 97%), and *n*-hexane (> 95%) were obtained from Sigma-Aldrich.

### Preparation of TFC membranes

The TFC-RO membrane was synthesized via an interfacial polymerization reaction of the aqueous phase of mPD with the organic phase of TMC on the porous PSf substrate according to the previously reported method [28, 37, 38]. First, the PSf support was prepared by phase inversion. A PSf solution (15% weight) was prepared by dissolving PSf pellets in DMF/NMP (4:1) mixture at 65 °C by 2 h. DMF was used as principal solvent, and NMP was used as pore former agent [28, 42]. After, the PSf casting solution obtained was uniformly dispersed on a glass plate using a casting knife with the knife gap set at 200  $\mu\text{m}$ . Next, the support was immersed in water as coagulation bath at room temperature. This support was recovered from the coagulation bath after 1 min and washed thoroughly with distilled water to remove any residual solvent. This PSf support was used for the TFC membrane preparation. The TFC-RO membrane was then synthesized via an interfacial polymerization reaction. The PSf support was immersed horizontally in a 2 wt% mPD aqueous solution containing 0.05 wt% NaOH during 2 min. The excess mPD was removed using a delicate task wiper (Kimwipes). Next, the membrane was immersed horizontally in a 0.2 wt% TMC solution in hexane for 1 min in order to allow the interfacial polymerization to occur. The resulting membrane was subsequently cured in an air circulation oven at 75 °C for 8 min. Finally, the resulting TFC membrane (PA/PSf) was washed with distilled water and dried at room temperature for 24 h.

### In situ formation of Cu-mPD oligomer complex within TFC membranes

The modified membrane (PA- $\text{CuCl}_2$ /PSf) was prepared by in situ Cu-mPD oligomer complex incorporation. First, a mixture ( $\text{Cu}^{2+}$  + mPD) was prepared adding  $\text{CuCl}_2$  salt (1.0 wt%) in mPD aqueous solution (2 wt%) containing 0.05 wt% sodium hydroxide (NaOH). During this process, a gradual change in the color of solution from colorless to dark brown with a small amount of solid material was observed. After, the PSf support was immersed horizontally in the mixture ( $\text{Cu}^{2+}$  + mPD) and it was kept in contact for 2 h. The excess mPD solution on its surface was removed using a delicate task wiper (Kimwipes). Next, the membrane was horizontally

immersed in a 0.2 wt% TMC solution in hexane for 1 min in order to allow interfacial polymerization. The resulting membrane was subsequently cured, washed, and dried followed by the procedure described in “Preparation of TFC membranes” section.

### Characterization of Cu-mPD oligomer complex

Fourier transform infrared spectroscopy (FTIR, Bruker Vector-22 Spectrophotometer, 250–4000  $\text{cm}^{-1}$ , KBr pellets) and ultraviolet–visible (UV–Vis) spectroscopy (Spectrophotometer HACH—DR-500, DMF solution) were used to identify the functional groups of the solid material formed during the mixture of  $\text{Cu}^{2+}$  + mPD that was used for the membrane modification.

### Characterization of membranes

Attenuated total reflectance Fourier transform infrared spectroscopy (ATR-FTIR [Model iS10, Nicolet]) was used to identify the functional groups in the dense PA layers of the membranes. X-ray diffraction (XRD) analyses were used to know the crystallinity of copper species present in the modified membrane (Bruker, D8 Advance,  $\text{CuK}\alpha 1$ , 40 kV/30 mA); the patterns were measured for  $2\theta$  values of  $0^\circ$ – $90^\circ$ . X-ray photoelectron spectroscopy (XPS) was used to determine chemical states of elements within the PA layer of modified and unmodified membranes. XPS spectra were recorded on an XPS-Auger PerkinElmer electron spectrometer Model PHI 1257 with an ultrahigh vacuum chamber, a hemispherical electron energy analyzer, and an X-ray source that provided unfiltered  $K_\alpha$  radiation from its aluminum anode ( $h\nu = 1486.6$  eV). The pressure of the main spectrometer chamber during data acquisition was  $10^{-7}$  Pa. The binding energy scale was calibrated using the peak from adventitious carbon, which was set to 284.6 eV. The membrane morphologies (cross-sectional) were studied using scanning electron microscopy (SEM) (INSPECT F-50, FEI Co.). The membranes were snapped under liquid nitrogen to give a generally consistent and clean cut. After that, the membranes were sputter-coated with a thin film of carbon to make them conductive. Elemental analyses were performed using energy-dispersive X-ray spectroscopy (EDS) (Model APOLLO-X, EDAX,

software Genesis V6.33), in order to confirm the presence of copper on the modified membrane. Additionally, the surface roughness of the membranes was investigated by using atomic force microscopy (AFM) in an AFM/STM Omicron Nanotechnology model SPM1 in contact mode. Surface roughness (RMS) of samples was calculated by using WSxM software over  $2500 \times 2500$   $\text{nm}^2$  images. The changes in membrane hydrophilicity were studied by contact angle measurements. Contact angles were measured by placing a sessile drop of ultrapure water on the membrane and performing drop shape analysis. Contact angle images were captured using a Digi-Microscope camera, a zoom lens of  $500\times$ , and a resolution of  $11 \mu\text{m}/\text{pixel}$ . Captured images were analyzed with the imaging processing software Image J. Three images were recorded per drop on a membrane and averaged.

### Antibiofouling tests

#### Bactericidal test

The bactericidal properties of the unmodified and modified membranes were evaluated by the colony-forming unit (CFU) method using *Escherichia coli* as the model gram-negative bacteria. This test was developed according to the previously reported method [28, 37, 38].

Bacteria were first cultured in tryptone soya broth (TSB) solution (30 g/L) and incubated in a shaking incubator in 200 revolutions per minute (rpm) at  $30^\circ\text{C}$  overnight. The bacterial solution was centrifuged in order to remove the nutrients and then washed in phosphate-buffered saline (PBS). The prepared bacteria were diluted 100 times in PBS to obtain a bacterial concentration of about  $1 \times 10^7$  cell/mL. Previously, the membrane samples were cut into squares of  $2 \times 2$   $\text{cm}^2$  and sterilized by ultraviolet radiation for 30 min. After that, each membrane piece was immersed separately in 10 mL prepared bacteria solution. Bacterial suspensions with membranes were incubated in a shaking incubator at  $30^\circ\text{C}$  for 4 h. At the same time, a 10-mL bacterial solution without a membrane was incubated as a control. After that, the treated solutions were serially diluted with PBS. From the highest dilution, 50  $\mu\text{L}$  of the solution was pipetted onto LB agar plates and then spread over the entire surface. The agar plates were incubated at  $35^\circ\text{C}$  overnight and were observed for developed

colonies in order to estimate the number of viable *E. coli* remaining in the suspensions.

### Antiadhesion test

The degree of bacterial attachment to the membrane surfaces was also assessed with *E. coli* according to the reported methodology [28]. The bacteria were prepared in the same manner as the bactericidal tests. Three pieces of each type of membrane (unmodified and modified) with an area of 2 cm<sup>2</sup> were incubated in the bacterial suspension at 30 °C while being shaken at 200 rpm. After incubation for 4 h, the membranes were removed from the suspension and gently rinsed with a 0.85 wt% NaCl solution in water. For total staining of cells on the membranes, they were stained with 1 µg/mL 4',6-diamidino-2-phenylindole. Dyes were added to the top surface of the membrane and incubated for 15 min in the dark. After incubation, the stained cells were observed under the epifluorescence microscope (Zeiss, Axio-Lab A1, Germany) with a 100× objective and were counted to estimate the number of cells that had adhered on the top surface of the membrane.

### Desalination performance test

Membranes performance was evaluated in terms of the permeate flux and salt rejection by using a cross-flow test cell with an effective area of 33 cm<sup>2</sup> and a feed solution of 1000 mg/L NaCl at 300 psi, following previous report [37, 38, 43]. The permeate flux test of membranes during 60 min was calculated by Eq. (1) [37, 38, 44]:

$$J = V/A \Delta t, \quad (1)$$

where  $J$  (L m<sup>-2</sup> h<sup>-1</sup>) is the membrane flux,  $V$  (L) is the volume of permeated water,  $A$  (m<sup>2</sup>) is the membrane area, and  $\Delta t$  (h) is the permeation time. The experiments were carried out at a temperature of 25 ± 1 °C. Additionally, solute rejection was measured from the feed and permeate solution concentrations by Eq. (2) [45]:

$$\text{Rejection} = \frac{C_f - C_p}{C_f} \times 100, \quad (2)$$

where  $C_f$  and  $C_p$  are the concentrations of the feed solution and permeate solution, respectively. The concentrations of these two solutions were obtained by their respective conductivity measurements.

### Copper and total organic carbon leaching cross-flow studies

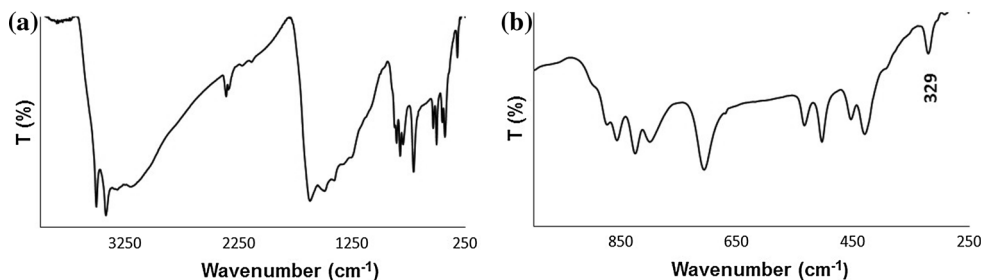
Copper concentrations in permeate water were measured in order to evaluate its stability on the membrane, verify Cu<sup>2+</sup> ions release, and determine a possible potential hazard of water quality. Moreover, the total organic carbon (TOC) was measured in order to determinate possible organic residue release from the Cu-mPD oligomer complex to the water permeate. The copper and organic carbon leaching studies were conducted using cross-flow experiments. A collection bottle to collect the permeate solution, which has passed over the copper charged membrane, was used. Samples were collected at different times of permeate flow. Copper concentration was analyzed by inductively coupled plasma optical emission spectrometry (ICP-OES, PerkinElmer, 7300 V) [37]. On the other hand, TOC was measured by Method 10173 using a DRB 200 reactor and ultraviolet-visible (UV-Vis) spectroscopy (Spectrophotometer HACH—DR-500, program 425 Organic Carbon MR).

## Results and discussion

### Characterization of Cu-mPD oligomer complex formed in situ within TFC membranes

The UV-Vis spectrum of the solid material collected from the complex formed in situ within a TFC membrane showed a broad peak at 447 nm (see Supplementary Material). It was attributed to Cu-mPD oligomer complex produced by coordination of Cu<sup>2+</sup> ions with the nitrogen atom of an aromatic amine [39, 41]. Moreover, the FTIR spectrum of this solid material showed a broad absorption between 3500 and 3000 cm<sup>-1</sup> corresponding to the stretching mode of NH [40] (Fig. 1). Additionally, peaks at 1620 and 1487 cm<sup>-1</sup> were associated with quinoid imine and benzenoid amine structures, respectively (Fig. 1). The peaks at 1253 and 329 cm<sup>-1</sup> corresponded to the Cu-N bond of the Cu-mPD oligomer complex, respectively [40]. Therefore, UV-Vis and FTIR characterization of solid material in the mixture (Cu<sup>2+</sup> + mPD) obtained during the first step of the membrane modification process suggests in situ formation of a Cu-mPD oligomer complex. The

**Figure 1** FTIR spectra of oligomer Cu-mPD complex: **a** complete spectrum, **b** zoom of spectrum (1000–250)  $\text{cm}^{-1}$ .



formation of a Cu-mPD oligomer complex from copper salts has been reported, and it appears to be due to the chelation capability of mPD with  $\text{Cu}^{2+}$ . Moreover, it is known that the redox reaction between  $\text{Cu}^{2+}$  and mPD produces oligomers [39, 40].

### Membrane characterization

The FE-SEM image of cross sections of the PA- $\text{CuCl}_2$ /PSf membrane is shown in Fig. 2. The image shows the formation of an ultrathin PA layer over the PSf support. Additionally, this PSf support contains long, finger-like voids extending from the top to the bottom of the substrate cross section, which are characteristic of PSf membranes synthesized by the phase inversion method [28, 37, 38]. Furthermore, SEM-EDX analyses of the PA- $\text{CuCl}_2$ /PSf membrane surface showed the presence of copper on the membrane surface (see in Supplementary Material), which can be attributed to the Cu-mPD oligomer complex formed during the synthesis of the polyamide layer.

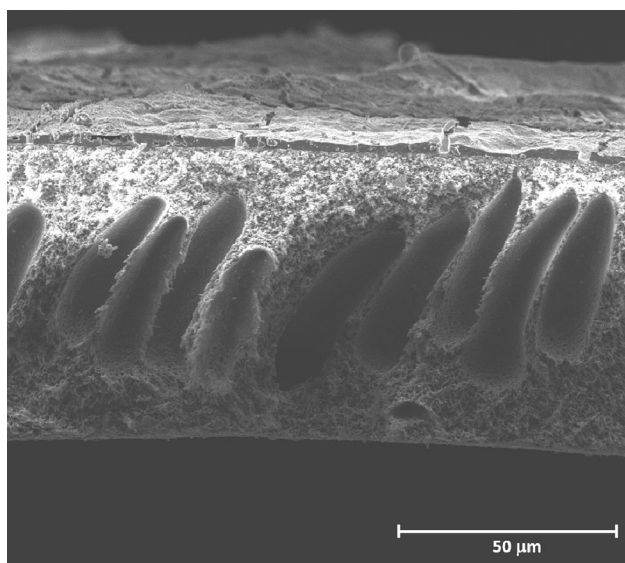


**Figure 2** FE-SEM image of cross section of modified membrane.

Moreover, FTIR-ATR spectroscopy was performed to identify functional groups on the surfaces of the membranes. Figure 3 shows the FTIR-ATR spectra of the unmodified and modified membranes, PA/PSf and PA- $\text{CuCl}_2$ /PSf, respectively. Both spectra exhibited weak peaks at approximately 1610 and 1680  $\text{cm}^{-1}$ ; these were attributed to amide bands [46, 47]. The band at  $\sim 1610 \text{ cm}^{-1}$  is characteristic of the PA aromatic ring, while the band at  $\sim 1680 \text{ cm}^{-1}$  corresponds to the C=O stretching vibration of PA. In addition, peaks were observed at 1405 and 1363  $\text{cm}^{-1}$ ; these correspond to the stretching vibrations of the  $-(\text{C}-\text{N})-$  and  $-(\text{C}-\text{O})-$  bonds in the polymer chain, respectively [48]. One peak observed at 2959  $\text{cm}^{-1}$  is attributed to aliphatic CH stretching [47]. Thus, it was confirmed that PA layers were successfully formed on the PSf support via interfacial polymerization even after the modification by the incorporation of the Cu-mPD oligomer complex.

Additionally, the FTIR-ATR spectrum of modified membranes showed one broad peak at 3200  $\text{cm}^{-1}$  corresponding to the stretching mode of  $-\text{NH}-$  also observed in Cu-mPD oligomer complex from the initial characterized mixture. Moreover, an intense peak at  $\sim 1620 \text{ cm}^{-1}$  in the modified membrane spectrum compared to the unmodified membrane spectrum was observed. This was attributed to the presence of the quinoid imine structure from Cu-mPD oligomer complex that was incorporated into the PA layer.

Moreover, chemical states of the elements within the PA layer of modified and unmodified membranes were determined by XPS. XPS spectra of unmodified membranes showed C 1s, O 1s, and N 1s peaks that were characteristic signals for the PA structure (see Supplementary Material) [49]. A full-range XPS spectra of the modified membranes showed C 1s, O 1s, N 1s, Cl 2p, and Cu 2p peaks (Fig. 4a). XPS results in concordance with FTIR analysis confirmed the incorporation of the Cu-mPD oligomer complex

**Figure 3** ATR-FTIR spectra of the membranes.

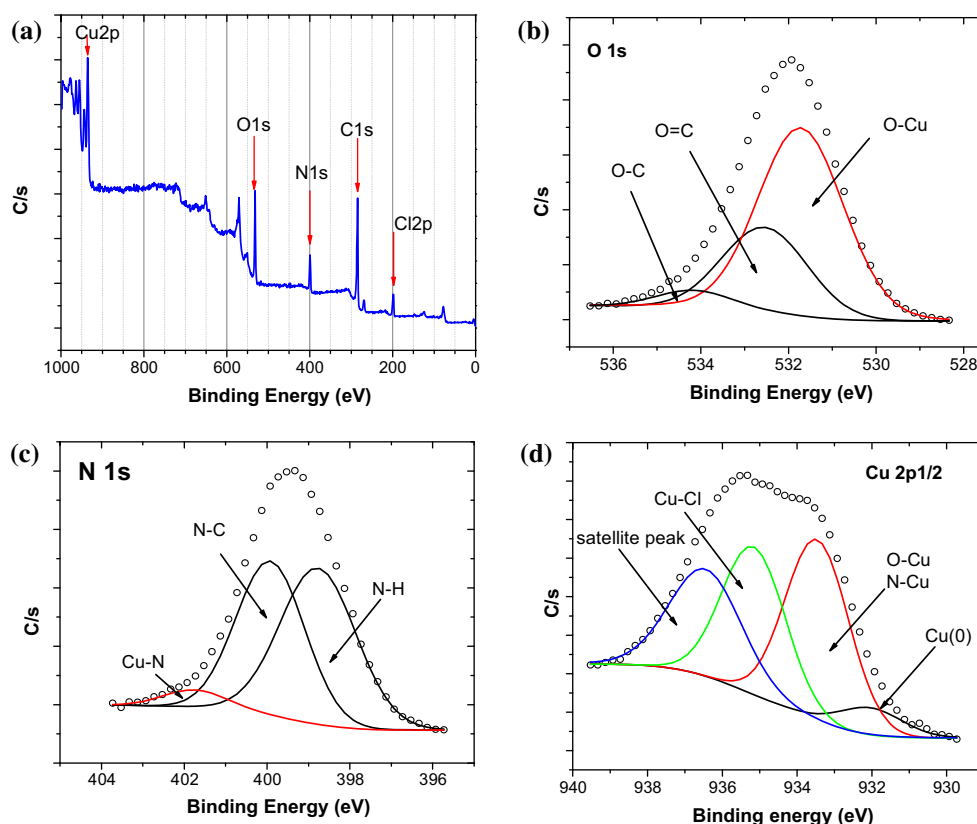
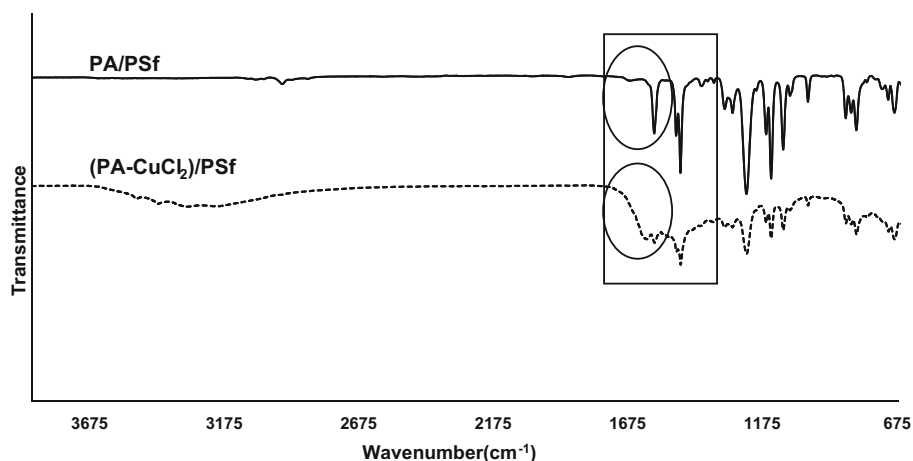


**Figure 4** XPS spectrum of modified membrane (PA-CuCl<sub>2</sub>)/PSf. **a** Full XPS spectra, **b** O 1s spectra, **c** N 1s spectra, **d** Cu 2p 1/2 spectra.

during interfacial polymerization without affecting the PA layer formation on the PSf support.

Numerical analysis of the C 1s spectrum of (PA-CuCl<sub>2</sub>)/PSf showed signals that are characteristic of the PA structure at 284.4, 287.2, and 289.5 eV, which could be attributed to C-C/C=C, O=C-N, O=C-O groups, respectively [49]. Additionally, one signal at 285.8 indicated the presence of C-N bonds present in both the PA layer and Cu-mPD oligomer complex

[41]. The XPS spectrum of O 1s (Fig. 4b) showed peaks at 532.5 and 534.2 eV corresponding to C=O and C-O groups in the PA, respectively [49]. Also, a signal at 531.7 eV was observed suggesting the presence of one interaction consisting of Cu-O=C [50].

On the other hand, numerical analysis of N 1s spectra showed the presence of N-H (398.7 eV) and N-C (399.9 eV) groups in the PA structure and

the protonated  $-N^+$  = quinoid imine units (401.7 eV) produced due to chelation of amino groups with  $Cu^{2+}$  (Fig. 4c) [49, 51]. The quinoid structure confirmed the formation of Cu-mPD oligomer complex into the PA layer. Additionally, the Cu  $2p_{1/2}$  spectrum showed peaks at 935.1 and 932.2 eV corresponding to Cu-Cl and Cu bonds, respectively (Fig. 3d) [52]. A third signal at 933.5 eV was observed in the Cu  $2p_{1/2}$  spectrum. This signal could be attributed to Cu-N and Cu-O bonds, suggesting the presence of the Cu-mPD complex and one possible interaction of Cu-O with the oxygen atoms of nascent polyamide carbonyl groups during the polymerization interfacial process.

Finally, X-ray diffraction (XRD) was analyzed in order to verify the crystallinity of copper species present in the modified membrane. XRD patterns of unmodified and modified membranes are shown in Fig. 5. One broad peak can be observed in both patterns located at  $10^\circ$ – $30^\circ$ , which is a typical characteristic for amorphous structure. The absence of peaks in the range of  $14^\circ$ – $68^\circ$  suggests the absence of crystallinity of copper species as Cu,  $Cu_2O$ , and CuO [53]. This fact would indicate that  $Cu^{2+}$  can be chelated to mPD as was also confirmed by XPS analyses. These results are in concordance with previous work related to the synthesis of Cu-poly-*m*-phenylenediamine (Cu-PmPD) nanocomposite which observed similar behavior [40].

Based on the previously described facts, a synthesis pathway for the in situ incorporation of the Cu-mPD oligomer complex into polyamide layer is shown in Scheme 1.

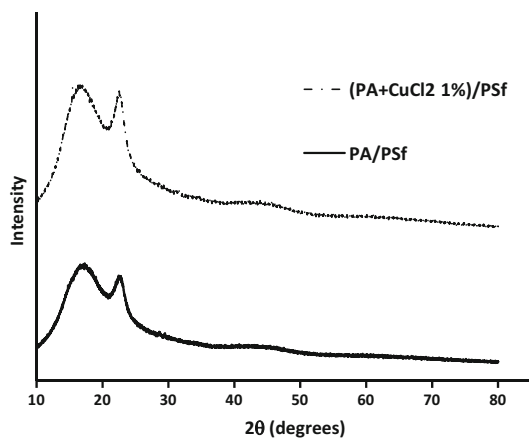


**Figure 5** XRD patterns of modified and unmodified membranes.

Thus, when  $CuCl_2$  is added to the mPD solution, one fraction of the mPD reacts with  $Cu^{2+}$  ions to produce a Cu-mPD oligomer complex due to the chelation capability of mPD with  $Cu^{2+}$ , and the other mPD fraction remains in solution (step 1). After that, this mPD in the solution reacts with the TMC via interfacial polymerization process in the presence of Cu-mPD oligomer complex (step 2). This Cu-mPD oligomer complex is self-assembled with the PA layer during interfacial polymerization process (step 3). It could be explained by an interaction via coordination between copper ions of the Cu-mPD oligomer complex and oxygen atoms of the carbonyl groups of the nascent PA layer ( $Cu-O=C$ ). This fact was confirmed by one observed signal at 531.7 eV in O 1s spectrum (XPS) of the modified membrane.

Surface membrane parameters such as roughness and hydrophilicity were studied by AFM and contact angle techniques, respectively. AFM images show that the top surfaces of the membranes exhibit characteristics consistent with those of interfacially polymerized polyamide membranes, which consist of ridge-and-valley layers (Fig. 6) [54, 55]. Furthermore, changes in surface membrane roughness are clearly observed in the modified membrane (Fig. 6b) in comparison with unmodified membranes (Fig. 6a).

The root-mean-square roughness parameter has been increased for a modified membrane compared with an unmodified membrane (Table 1). Thus, it can be noted that the in situ formation of the Cu-mPD oligomer complex in the membrane during the interfacial polymerization process significantly increases the surface roughness. This effect can be attributed to changes in polymer growth due to the presence of the Cu-mPD oligomer complex during the interfacial polymerization process, which affects the height between ridges and valleys of the PA layer and increases its surface roughness. In contrast, other ways of modifying TFC-RO membranes have been reported: (1) PA functionalization with Cu nanoparticles by dip coating [19] and (2) in situ surface functionalization with Cu-NPs formed on the surfaces of commercial TFC-RO membranes [32]. Neither modification method causes significant changes in surface roughness.

It is known that increase in surface roughness could influence the antibiofouling effects because more biofoulants are likely to be entrapped in membranes with rougher topologies [1, 28].



**Scheme 1** Mechanism of formation of modified membranes with Cu-mPD oligomer complex.

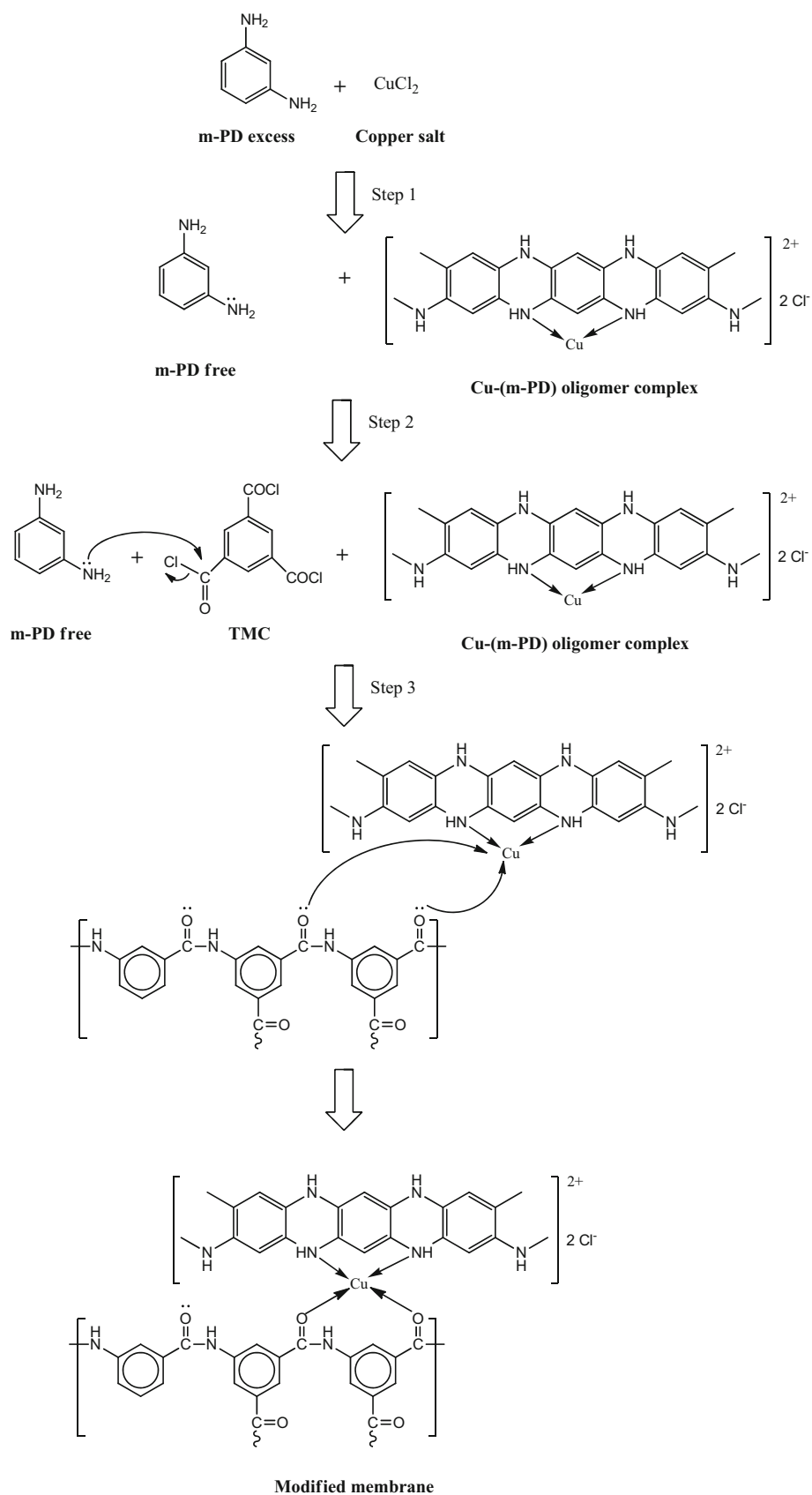


**Figure 6** AFM scan of the membranes. **a** PA/PSf, **b** (PA-CuCl<sub>2</sub>)/PSf.

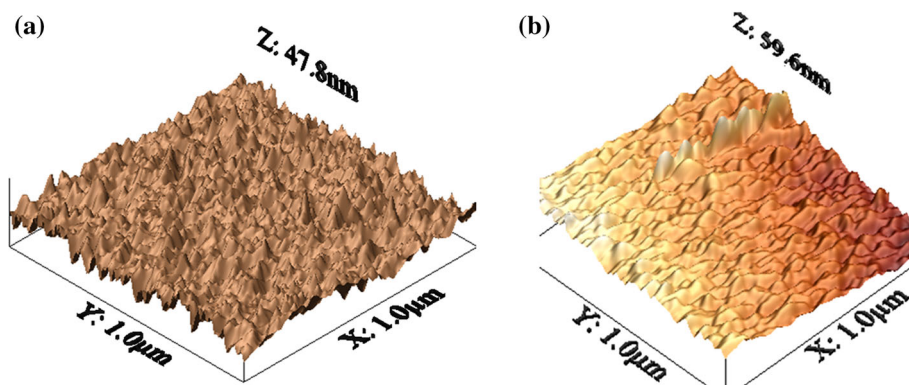


**Table 1** Surface parameters of membranes

Membrane	Root-mean-square roughness (RMS) of membranes studied (nm)	Contact angle
PA/PSf	18 ± 4	68 ± 2
(PA-CuCl <sub>2</sub> )/PSf	52 ± 6	74 ± 2

On the other hand, Cu-mPD oligomer complex incorporation within the PA membrane layer forms a slightly less hydrophilic surface. Thus, an increase in the contact angle from  $68^\circ \pm 2^\circ$  to  $74^\circ \pm 2^\circ$  in unmodified and modified membranes, respectively, was observed (Fig. 7, Table 1). A similar behavior was observed by Ben-Season in modified membrane surfaces formed with copper nanoparticles by in situ functionalization of the PA layer [32].

### Antibiofouling effect

The number of *E. coli* colonies formed in the medium in the presence of a modified membrane was significantly lower in comparison with an unmodified membrane (Table 2). Therefore, an important bactericidal effect due to membrane modification was observed. Thus, the reduction in the number of CFUs in the aqueous medium in the presence of modified membrane was 99% compared to unmodified membrane.

Moreover, the numbers of bacteria adhering to the modified membrane surfaces were significantly lower ( $260 \text{ cell/mm}^2$ ) with respect to unmodified membrane surfaces ( $26375 \text{ cell/mm}^2$ ) (Table 2). Thus, a significant antiadhesion capacity on modified membranes was observed compared to unmodified membranes.

Although no favorable changes on the surface physicochemical properties of modified membranes with respect to unmodified membrane were observed (slightly less hydrophilic and more roughness surface), excellent bactericidal and antiadhesion effects were observed in the presence of this modified membrane, which was mainly attributed to copper toxicity.

Bacteria can be inactivated due to the Cu-mPD oligomer complex acting as source of Cu<sup>2+</sup> ions biocide release into the boundary layer above the membrane to form an inhibition zone [7, 19, 20]. Similar N-polymer-copper complexes and amine-copper complexes employed to modified membranes

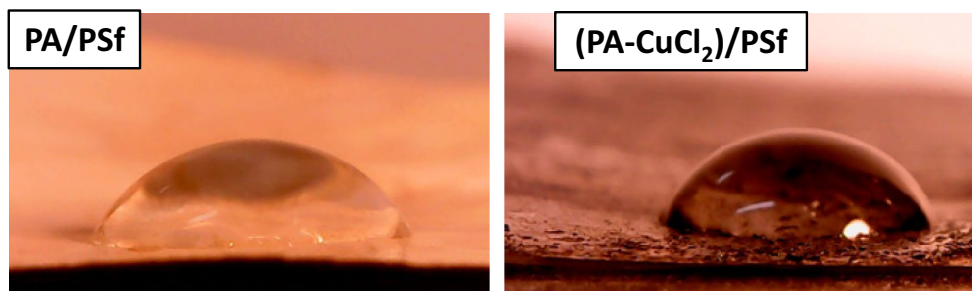


**Figure 7** Images of water drop on membrane studied.

**Table 2** Antibiofouling properties of membranes

Membrane	CfU/mL	Number of cell adhered on surface (cell/mm <sup>2</sup> )
PA/PSf	$10.0 \times 10^7$	26375
(PA-CuCl <sub>2</sub> )/PSf	$8.0 \times 10^4$	260

and other matrixes have demonstrated this same behavior [56, 57]. Cu<sup>2+</sup> ions released from the Cu-mPD oligomer complex have toxic effects on bacteria in the medium because these ions trigger the production of reactive oxygen species, which damage the DNA of the bacteria, thus killing them [18]. Moreover, these biocidal ions would form an inhibitory zone around the membrane and reduce the number of CFUs in the aqueous medium leading to a decrease in the number of bacteria that could potentially attach to the membrane surface [18].

### Desalination performance

The modified membrane showed an important salt rejection of about 97% with stable water flux for 60 min and a recovery of 50% similar to unmodified membrane (Table 3). Additionally, modified membrane presented a permeate flux of  $1.6 \text{ L m}^{-2} \text{ h}^{-1} \text{ bar}^{-1}$  which is 1.3 times higher with respect to unmodified membrane, indicating that the modification with Cu-mPD oligomer into membrane promotes an increase in the permeate flux on the membrane. A similar behavior was observed on reverse osmosis membrane modified with CuO nanoparticles [38] attributed to the hydrophilic character of these nanoparticles [31, 38].

### Copper and total organic carbon (TOC) leaching cross-flow studies

In order to evaluate the modified membrane stability and Cu<sup>2+</sup> release in the treated water, copper concentration from the cross-flow leaching experiments was determined and is shown in Table 4.

It can be noted that copper concentration in the permeate solution increases at long operation time; however, the maximum values observed were around 0.363 mg/L, which can be considered

negligible, according to the World Health Organization (WHO) [58] (copper concentration limit < 2 mg/L). Moreover, a non-gradual release of copper ions in the operation times was observed.

Previous studies on membrane modification with copper nanoparticles and copper complexes have also shown a non-gradual increase in copper concentration in the permeate water with increases at operation times. In addition, they have shown that after a certain operation time, a maximum concentration of leached copper can be reached, which would remain constant. This maximum time can be reached on minutes [37] or days [56], depending on the modification and the type of membrane.

Thus, future studies should be conducted to explore the time in which this equilibrium is reached and the values of the maximum copper concentration observed, in order to predict the lifetime of the membrane and the efficiency antibiofouling property in a long operation time.

Additionally, TOC measurement was taken in order to estimate the impact that would produce the release of Cu-mPD oligomer in the amount of organic material into permeate water. The TOC concentrations showed values below 0.5 mg/L which can be considered negligible, according to the EPA Drinking Water Regulation.

### Conclusions

A novel synthesis method to obtain modified TFC-RO membranes with Cu-mPD oligomer complexes was achieved. The method consists of in situ formation of a Cu-mPD oligomer complex from copper chloride during the IPP. Several characterization techniques (FTIR, XPS, XRD) demonstrated the formation of Cu-mPD oligomer complexes due to interactions between Cu<sup>2+</sup> ions and mPD during IPP.

**Table 3** Permeate flux and rejection of salts percentage of the membranes

Membrane	Flux permeate ( $\text{L m}^{-2} \text{ h}^{-1} \text{ bar}^{-1}$ )	Rejection of salts percentage (%)
PA/PSf	$1.2 \pm 0.1$	$96.9 \pm 0.2$
(PA-CuCl <sub>2</sub> )/PSf	$1.6 \pm 0.1$	$97.3 \pm 0.2$

**Table 4** Concentrations of copper and total organic carbon in the permeated flux by using modified membrane

Permeate time (min)	Copper concentration (ppb)	Total organic carbon concentration (ppm)
45	87.1 ± 0.2	< 0.5
90	213.0 ± 0.2	< 0.5
120	363.0 ± 0.2	< 0.5

Moreover, the incorporation mechanism for the Cu-mPD oligomer complex within the PA layer has been proposed as an interaction between copper ions of the Cu-mPD oligomer complex and oxygen atoms of the carbonyl groups of the nascent PA layer produced during IPP. The modification produced a slight decrease in membrane hydrophilicity and higher surface roughness of modified membranes compared to unmodified membranes. These features did not affect the antibiofouling properties of modified membranes. In fact, the PA-CuCl<sub>2</sub>/PSf membrane showed excellent antibiofouling properties with a decrease of 99% in CFUs compared to unmodified membranes. Bacterial adherence was also significantly lower (260 cell/mm<sup>2</sup>) compared to unmodified membranes (26375 cell/mm<sup>2</sup>) when *E. coli* was used as the bacterial model. This behavior was attributed to copper ion toxicity as a result of Cu<sup>+2</sup> ions release from the membrane surface. In this context, release of copper ions in the permeate water was determined and the maximum value observed was considered negligible for according to the WHO. Finally, the desalination performance of modified membranes showed an important salt rejection with stable water flux.

In conclusion, a novel chemical method for the incorporation of Cu-mPD oligomer complex into the polyamide layer of TFC-RO membranes to improve their antibiofouling properties and desalination performance was achieved.

## Acknowledgements

The authors gratefully acknowledge financial support provided by National Fund for Scientific and Technological Development (FONDECYT) of the Government of Chile (Project No. 11130251). The authors thank Solvay Advanced Polymers for donating the polysulfone Udel P-1700. The authors also thank to the Water Quality Laboratory of the Department of Civil Engineering of Universidad de

Chile for giving the infrastructure and the technician Viviana Lorca for TOC measures made.

**Funding** This study was funded by National Fund for Scientific and Technological Development (FONDECYT) of the Government of Chile (Grant No. 11130251).

## Compliance with ethical standards

**Conflict of interest** The authors declare that they have not conflict of interest.

**Electronic supplementary material:** The online version of this article (<https://doi.org/10.1007/s10853-018-2039-4>) contains supplementary material, which is available to authorized users.

## References

- [1] Kang GD, Cao YM (2012) Development of antifouling reverse osmosis membranes for water treatment: a review. *Water Res* 46:584–600
- [2] Buonomenna MG (2013) Nano-enhanced reverse osmosis membranes. *Desalination* 314:73–88
- [3] Subramani Arun, Jacangelo Joseph G (2015) Emerging desalination technologies for water treatment: a critical review. *Water Res* 75:164–187
- [4] Gohil Jaydevsinh M, Ray Paramita (2017) A review on semi-aromatic polyamide TFC membranes prepared by interfacial polymerization: potential for water treatment and desalination. *Sep Purif Technol* 181:159–182
- [5] Ghosh AK, Bindal RC, Prabhakar S, Tewari PK (2011) Composite polyamide reverse osmosis (RO) membranes—recent developments and future directions technology development. *BARC Newsl* 321:43–51
- [6] Jiang Shanxue, Li Yuening, Ladewig Bradley P (2017) A review of reverse osmosis membrane fouling and control strategies. *Sci Total Environ* 595:567–583
- [7] Karkhanechi H, Razi F, Sawada I, Takagi R, Ohmukai Y, Matsuyam H (2013) Improvement of antibiofouling performance of a reverse osmosis membrane through biocide

- release and adhesion resistance. *Sep Purif Technol* 105:106–113
- [8] Asatekin A, Mayes AM (2009) Oil industry wastewater treatment with fouling resistant membranes containing amphiphilic comb copolymers. *Environ Sci Technol* 43:4487–4492
- [9] Ong CS, Goh PS, Lau WJ, Misdan N, Ismail AF (2016) Nanomaterials for biofouling and scaling mitigation of thin film composite membrane: a review. *Desalination* 393:2–15
- [10] Kang GD, Cao YM (2012) Development of antifouling reverse osmosis membranes for water treatment: a review. *Water Res* 46:584–600
- [11] Buonomenna MG (2013) Nano-enhanced reverse osmosis membranes. *Desalination* 314:73–88
- [12] Guo-Rong Xu, Wang Jiao-Na, Li Cong-Ju (2013) Strategies for improving the performance of the polyamide thin film composite (PA-TFC) reverse osmosis (RO) membranes: surface modifications and nanoparticles incorporations. *Desalination* 328:83–100
- [13] Lia Xin, Sotto Arcadio, Li Jiansheng, Van der Bruggen Bart (2017) Progress and perspectives for synthesis of sustainable antifouling composite membranes containing in situ generated nanoparticles. *J Membr Sci* 524:502–528
- [14] Kango S, Kaliab S, Celli A, Njugunad J (2013) Surface modification of inorganic nanoparticles for development of organic–inorganic nanocomposites—a review. *Prog Polym Sci* 38:1232–1261
- [15] Kim J, Van der Bruggen B (2010) The use of nanoparticles in polymeric and ceramic membrane structures: review of manufacturing procedures and performance improvement for water treatment. *Environ Pollut* 158:2335–2349
- [16] Goh PS, Ismail AF (2015) Review: Is interplay between nanomaterial and membrane technology the way forward for desalination? *J Chem Technol Biotechnol* 90:971–980
- [17] Goh PS, Ismail AF, Hilal N (2016) Nano-enabled membranes technology: sustainable and revolutionary solutions for membrane desalination? *Desalination* 380:100–104
- [18] Karkhanechi H, Razi F, Sawada I, Takagi R, Ohmukai Y, Matsuyama H (2013) Improvement of antibiofouling performance of a reverse osmosis membrane through biocide release and adhesion resistance. *Sep Purif Technol* 105:106–113
- [19] Ben-Sasson M, Zodrow K, Genggeng Q, Kang Y, Giannelis E, Elimelech M (2014) Surface functionalization of thin-film composite membranes with copper nanoparticles for antimicrobial surface properties. *Environ Sci Technol* 48:384–393
- [20] Banerjee I, Pangule RC, Kane RS (2011) Antifouling coatings: recent developments in the design of surfaces that prevent fouling by proteins, bacteria, and marine organisms. *Adv Mater* 23:690–718
- [21] Cioffi N, Torsi L, Ditaranto N, Tantillo G, Ghibelli L, Sabbatini L, Bleve-Zacheo T, D'Alessio M, Zamboni P, Traversa E (2005) Copper nanoparticle/polymer composites with antifungal and bacteriostatic properties. *Chem Mater* 17:5255–5262
- [22] Chapman JS (2003) Biocide resistance mechanisms. *Int Biodeterior Biodegradation* 51:133–138
- [23] Bagchi B, Dey S, Bhandary S, Das S, Bhattacharya A, Basu R, Nandy P (2012) Antimicrobial efficacy and biocompatibility study of copper nanoparticle adsorbed mullite aggregates. *Mater Sci Eng C32*:1897–1905
- [24] Ren G, Hu D, Cheng EW, Vargas-Reus MA, Reip P, Allaker RP (2009) Characterisation of copper oxide nanoparticles for antimicrobial applications. *Int J Antimicrob Agents* 33:587–590
- [25] Baek YW, An YJ (2011) Microbial toxicity of metal oxide nanoparticles (CuO, NiO, ZnO, and Sb<sub>2</sub>O<sub>3</sub>) to *Escherichia coli*, *Bacillus subtilis*, and *Streptococcus aureus*. *Sci Total Environ* 409:1603–1608
- [26] Bondarenko O, Juganson K, Ivask A, Kasemets K, Mortimer M, Kahru A (2009) Toxicity of nanoparticles of CuO, ZnO and TiO<sub>2</sub> to microalgae *Pseudokirchneriella subcapitata*. *Sci Total Environ* 407:1461–1468
- [27] Shaffiey SF, Bozorgnia A, Ahmad M (2014) Synthesis and evaluation of bactericidal properties of CuO nanoparticles against *Aeromonas hydrophila*. *Nanomed J* 1:98–204
- [28] García A, Quintero Y, Vicencio N, Rodríguez B, Öztürk D, Mosquera E, Corrales TP, Volkmanf Elimelech UG (2016) Influence of TiO<sub>2</sub> nanostructures on anti-adhesion and photoinduced bactericidal properties of thin film composite membranes. *RSC Adv* 6:82941–82948
- [29] Akar N, Asar B, Dizge N, Koyuncu I (2013) Investigation of characterization and biofouling properties of PES membrane containing selenium and copper nanoparticles. *J Membr Sci* 437:216–226
- [30] Isloor A, Ganesh BM, Isloor S, Ismail AF, Nagaraj HS, Pattabi M (2013) Studies on copper coated polysulfone/modified poly isobutylene alt-maleic anhydride blend membrane and its antibiofouling property. *Desalination* 308:82–88
- [31] Baghbanzadeh M, Rana D, Matsuura T, Lan C (2015) Effects of hydrophilic CuO nanoparticles on properties and performance of PVDF VMD membranes. *Desalination* 369:75–84
- [32] Ben-Sasson M, Lu X, Nejati S, Jaramillo H, Elimelech M (2016) In situ surface functionalization of reverse osmosis membranes with biocidal copper nanoparticles. *Desalination* 38:1–8

- [33] Hausman R, Gullinkala T, Escobar IC (2010) Development of copper-charged polypropylene feedspacers for biofouling control. *J Membr Sci* 35:114–121
- [34] Hausman R, Gullinkala T, Escobar IC (2009) Development of low-biofouling polypropylene feedspacers for reverse osmosis. *J Appl Polym Sci* 114:3068–3073
- [35] Xu J, Feng X, Chen P, Gao C (2012) Development of an antibacterial copper (II)-chelated polyacrylonitrile ultrafiltration membrane. *J Membr Sci* 413–414:62–69
- [36] Asapu S, Pant S, Gruden CL, Escobar IC (2014) An investigation of low biofouling copper-charged membranes for desalination. *Desalination* 338:17–25
- [37] Garcia A, Rodríguez B, Oztürk D, Rosales M, Paredes C, Cuadra F, Montserrat S (2016) Desalination performance of antibiofouling reverse osmosis membranes. *Mod Environ Sci Eng* 2:481–489
- [38] García A, Rodríguez B, Oztürk D, Rosales M, Diaz DI, Mautner A (2017) Incorporation of CuO nanoparticles into thin-film composite reverse osmosis membranes (TFC-RO) for antibiofouling properties. *Polym Bull* 46:1–17
- [39] Zhang L, Wang H, Yu W, Su Z, Chai L, Li J, Shi Y (2012) Facile and large-scale synthesis of functional poly(*m*-phenylenediamine) nanoparticles by Cu<sup>2+</sup>-assisted method with superior ability for dye adsorption. *J Mater Chem* 22:18244–18251
- [40] Da S, Peng B, Zhang L, Chai L, Wang T, Meng Y, Li X, Wang H, Luo J (2015) Sustainable synthesis of hollow Cu-loaded poly(*m*-phenylenediamine) particles and their application for arsenic removal. *RSC Adv* 5:29965–29974
- [41] Chai L, Wang T, Zhang L, Wang H, Yang W, Dai S, Meng Y, Li X (2015) A Cu-*m*-phenylenediamine complex induced route to fabricate poly(*m*-phenylenediamine)/reduced graphene oxide hydrogel and its adsorption application. *Carbon* 81:748–757
- [42] Rahimpour A, Madaeni SS, Taheri AH, Mansourpanah Y (2008) Coupling TiO<sub>2</sub> nanoparticles with UV irradiation for modification of polyethersulfone ultrafiltration membranes. *J Membr Sci* 313:158–169
- [43] Saleh TA, Gupta VK (2012) Synthesis and characterization of alumina nano-particles polyamide membrane with enhanced flux rejection performance. *Sep Purif Technol* 89:245–251
- [44] Zhang M, Zhang K, De Gussem B, Verstraete W (2012) Biogenic silver nanoparticles (bio-Ag 0) decrease biofouling of bio-Ag 0/PES nanocomposite membranes. *Water Res* 46(7):2077–2087
- [45] Lee HS, Im SJ, Kim JH, Kim HJ, Kim JP, Min BR (2008) Polyamide thin-film nanofiltration membranes containing TiO<sub>2</sub> nanoparticles. *Desalination* 219(1–3):48–56
- [46] Tang CY, Kwon Y-N, Leckie JO (2009) Effect of membrane chemistry and coating layer on physicochemical properties of thin film composite polyamide RO and NF membranes: I. FTIR and XPS characterization of polyamide and coating layer chemistry. *Desalination* 242:149–167
- [47] Akin O, Temelli F (2011) Probing the hydrophobicity of commercial reverse osmosis membranes produced by interfacial polymerization using contact angle, XPS, FTIR, FE-SEM and AFM. *Desalination* 278:387–396
- [48] Robert FXW, Silverstein M, Kiemle D (2005) Spectrometric identification of organic compounds, 7th edn. Wiley, New York
- [49] Khorshidi B, Soltannia B, Thundat T, Sadrzadeh M (2017) Synthesis of thin film composite polyamide membranes: effect of monohydric and polyhydric alcohol additives in aqueous solution. *J Membr Sci* 523:336–345
- [50] Hoof DL, Tisley DG, Walton RA (1973) Studies on metal carboxylates. Part III. Pyridine-2,6-dicarboxylates of the lanthanides. Synthesis and spectral studies and the X-ray photoelectron spectra of several pyridine carboxylate complexes. *J Chem Soc, Dalton Trans* 2:200–204
- [51] Zhang LY, Chai LY, Liu J, Wang HY, Yu WT, Sang PL (2011) pH manipulation: a facile method for lowering oxidation state and keeping good yield of poly (*m*-phenylenediamine) and its powerful Ag<sup>+</sup> adsorption ability. *Langmuir* 27:13729–13738
- [52] Wagner CD, Riggs WM, Davis LE, Moulder JF, Muilenberg GE (1979) Handbook of X-ray photoelectron spectroscopy, vol 190. Perkin-Elmer Corporation, Waltham
- [53] Liu Zhirong Md, Uddin Azhar, Zhanxue Sun (2011) FT-IR and XRD analysis of natural Na-bentonite and Cu(II)-loaded Na-bentonite. *Spectrochim. Acta Part A* 79:1013–1016
- [54] Porter MC (1991) Handbook of industrial membrane technology. Noyes Publications, Saddle River
- [55] Kwak SGJSY, Yoon YS, Ihm DW (1999) Details of surface features in aromatic polyamide reverse osmosis membranes characterized by scanning electron and atomic force microscopy. *J Polym Sci, Part B: Polym Phys* 37:1429–1440
- [56] Jia Xu, Zhang Lili, Gao Xueli, Bie Haiyan, Yunpeng Fu, Gao Congjie (2015) Constructing antimicrobial membrane surfaces with polycation-copper (II) complex assembly for efficient seawater softening treatment. *J Membr Sci* 494:28–36
- [57] Lupsea Maria, Mathies Helena, Schoknecht Ute, Tiruta-Barna Ligia, Schiopu Nicoleta (2013) Biocide leaching from CBA treated wood—a mechanistic interpretation. *Sci Total Environ* 444:522–530
- [58] Nadraroglu H, Kalkan E, Demir N (2010) Removal of copper from aqueous solution using red mud. *Desalination* 251:90–95